

Electronic Supplementary Information

Supramolecular architectures based on binuclear
Pt(II) complexes consisting different ligands;
circular and helical fiber structures

Minhye Kim,^a Mirae Ok,^a Chenxing Li,^a Kayeong Go,^a Sehee Kim,^a Juyeong Kim,^a Jong Hwa
Jung*^a and Sung Ho Jung*^a

*Department of Chemistry and Research Institute of Natural Sciences Gyeongsang National University,
Jinju 52828, Korea*

Contents

1. Method

1.1 General characterization	S3
1.2 UV-vis studies studies	S3
1.3 Preparation of platinum complexes	S3
1.4 AFM observation	S3
1.5 SEM observation	S3
1.6 Calculation of thermodynamic parameter	S4
1.7 Theoretical calculations	S4

2. Synthesis and characterization

2.1 Synthesis of <i>R-L</i> ²	S4
2.2 Synthesis of <i>R-L</i> ¹	S4
2.3 Synthesis of Ch-1	S5
2.4 Synthesis of Ph-1	S5
2.5 Synthesis of Py-1	S6

3. Supplementary scheme and figures

3.1 Scheme S1	S6
3.2 Figures S1-S26	S6
3.3 Tables S1-S2	S17

4. Analytical data

4.1 ¹ H- and ¹³ C-NMR spectra	S18
4.2 ESI mass spectra	S21

Supplementary data

1. Methods

1.1 General characterization: The ^1H and ^{13}C NMR spectra were taken on a Bruker DRX 300, and Bruker DRX 500. Mass spectroscopy samples were analyzed on a JEOL JMS-700 mass spectrometer. The high resolution mass spectra (HR-MS) were measured by electrospray ionization (ESI) with a micro TOF Focus spectrometer from SYNAPT G2 (Waters, U.K.). A UV-visible spectrophotometer (JASCO V-750) was used to obtain the absorption spectra. IR spectra were observed over the range $500\text{-}4000\text{ cm}^{-1}$, with a Thermo scientific Nicolet iS 10 instrument. Florescence lifetimes of **Ch-1** and **Ph-1** were measured at room temperature by C11367-11. Powder X-ray pattern (PXRD) was recorded on a Rigaku model NANOPIX X-ray diffractometer with a Cu K_α radiation source.

1.2 UV-vis studies: The UV-vis spectra were recorded on a JASCO V-750 UV-visible spectrophotometer. The UV-vis spectra were determined over the range of $200\text{-}700\text{ nm}$ using a quartz cell with 0.1 mm and 1 mm path length. Scans were taken at rate of 500 nm/min with a sampling interval of 0.5 nm and response time of 0.5 s . To elucidate the supramolecular polymerization process, **Ch-1** (9 mM) with or without pyridine, and **Ph-1** (9 mM) were dissolved in $\text{H}_2\text{O/DMSO}$ ($1:9\text{ v/v}$). After adding the sample to the UV cells, it was heated to 363 K ($1\text{ }^\circ\text{C/min}$) to form the monomeric species in UV-vis spectroscopy. Then the sample was cooled to 293 K ($1\text{ }^\circ\text{C/min}$) in UV-vis spectroscopy. The time-dependent UV-vis spectral changes were measured at 293 K .

1.3 AFM observation: Atomic force microscope (AFM) imaging was performed by using XE-100 and a PPP-NCHR 10 M cantilever (Park systems). The AFM samples were prepared by spin-coating (2000 rpm) onto freshly cleaved Muscovite Mica, and images were recorded with the AFM operating in noncontact mode in air at RT with resolution of 1024×1024 pixels, using moderate scan rates (0.3 Hz).

1.4 SEM observation: FE-SEM images were observed using a JEOL (JSM-7900F). The images of samples using an accelerating voltage 10 kV and an emission current of $8\mu\text{A}$. Samples were prepared by dropping dilute solution of supramolecular nanostructure formed in water on glasses following by spinning, drying and coating them with a thin layer of Pt to increase the contrast.

1.5 Calculation of thermodynamic parameter: The thermodynamic parameters governing

the supramolecular aggregation of **Ch-1** and **Ph-1** were obtained by the global fitting of the melting curves. This global fitting is performed by using the equilibrium (EQ) model reported by ten Eikelder and coworkers.¹ The values for the elongation enthalpy (ΔH_e) and the entropy (ΔS_e), and elongation binding constant (K_e) used in the cooperative supramolecular polymerization models were determined by the global fitting of the heating curves,²⁻⁴ which were obtained by plotting the degree of aggregation (α_{agg}) of **Ch-1** (9 mM) without or with pyridine (140 equiv.) and **Ph-1** (9 mM) at 331 nm against temperature with heating experiments. An elongation binding constant (K_e) for aggregation at 293 K was estimated according to equation 1, from which the enthalpy change (ΔH), and the entropy change (ΔS) were determined:

$$K_e = e^{-\frac{(\Delta H_e - T\Delta S_e)}{RT}} \quad (\text{equation 1})$$

2. Synthesis and characterization

2.1 Synthesis of *R-L*²: (*R*)-(-)-2-amino-1-propanol (0.28 g, 3.7 mmol) was added to a stirred suspension of powdered KOH (1.05 g, 18.7 mmol) in dry DMSO (20 mL) at 60 °C. After 30 min, 4'-chloro-2,2':6',2''-terpyridine (1.00 g, 3.7 mmol) was added to the mixture. The mixture was then stirred for 4 h at 70 °C and poured into 600 mL of distilled water thereafter. CH₂Cl₂ (3 × 200 mL) was used to extract the aqueous phase. Residual water in dichloromethane was dried over Na₂SO₄ and CH₂Cl₂ was removed in vacuum, and the desired product was purified by recrystallization with ethyl acetate to give 0.72 g (72%) of *R-L*². Mp = 118.3 °C; IR (KBr pellet): 3375, 2964, 2926, 2846, 1577, 1565, 1473, 1439, 1403, 1353, 1204, 799 cm⁻¹; ¹H NMR (300 MHz, CDCl₃): δ 8.70 (m, *J* = 4.8, 1.8, 0.9 Hz, 2H), 8.62 (m, *J* = 8.0, 1.1 Hz, 2H), 8.02 (s, 2H), 7.84 (m, *J* = 7.7, 1.8 Hz, 2H), 7.33 (m, *J* = 7.4, 4.8, 1.2 Hz, 2H), 4.14 (m, *J* = 9.0, 4.1 Hz, 1H), 3.94 (m, *J* = 9.1, 7.6 Hz, 1H), 3.41 (m, *J* = 10.6, 7.6, 6.6, 4.2 Hz, 1H), 1.21 (d, *J* = 6.5 Hz, 3H); ¹³C NMR (125 MHz, DMSO-*d*₆): δ 167.2, 157.1, 155.3, 149.7, 137.9, 125.0, 121.3, 107.3, 75.1, 46.2, 20.43; HR-Mass (*m/z*) calculated for C₁₈H₁₈N₄O [M]⁺: 306.3690, Found [M]⁺: 306.3690.

2.2 Synthesis of *R-L*¹: *R-L*¹ was prepared according to a literature procedure. In a two neck flask, *R-L*² (0.50 g, 1.64 mmol) and TEA (0.1 mL, 0.72 mmol) were added to dry CH₂Cl₂ (10 mL). After cooling the solution in an ice bath, sebacyl chloride (0.16 mL, 0.75 mmol) was

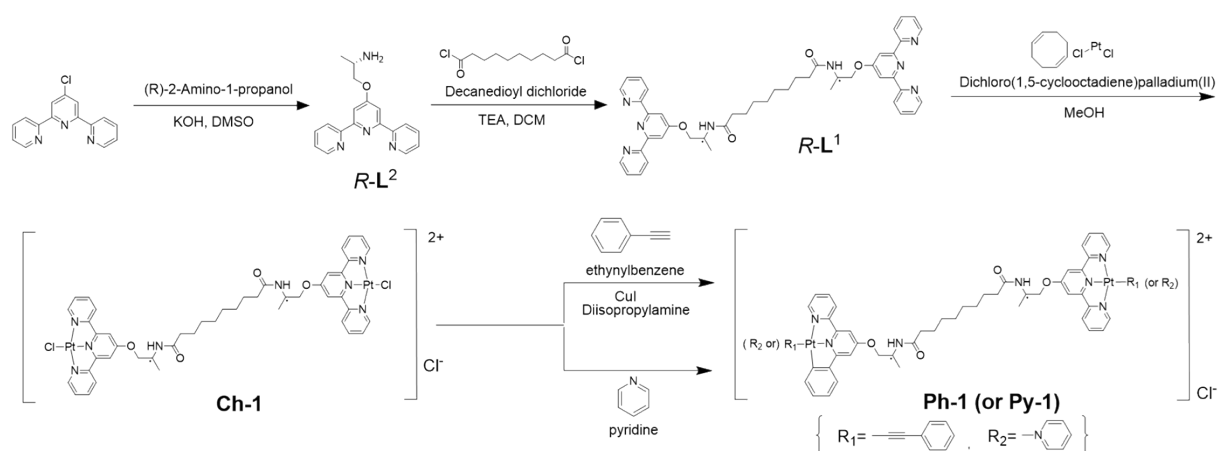
added dropwise. The reactant was stirred for 3 h at room temperature. The crude product was recrystallized from CH₂Cl₂ to give a white crystalline solid **R-L¹** in 49.7% yield (0.632 g). Mp = 198 °C; IR (KBr pellet): 3428, 3311, 2929, 2845, 1640, 1582, 1563, 1466, 1446, 1407, 1362, 1207, 1038, 785 cm⁻¹; ¹H NMR (300 MHz, DMSO-*d*₆): δ 8.68 (m, 8H), 7.99 (m, 8H), 7.87 (d, *J* = 7.5 Hz, 2H), 7.50 (m, *J* = 7.7, 4.8, 1.6 Hz, 4H), 4.15 (m, 6H), 2.02 (t, *J* = 7.3 Hz, 4H), 1.42 (d, *J* = 7.5 Hz, 4H), 1.21 (s, 3H), 1.19 (s, 3H), 1.13 (s, 8H); ¹³C NMR (125 MHz, DMSO-*d*₆): δ 172.3, 167.1, 157.2, 155.3, 149.7, 137.8, 125.0, 121.3, 107.2, 70.9, 44.1, 35.9, 29.2, 29.0, 25.7, 17.6; HR-Mass (m/z) calculated for C₄₆H₅₀N₈O₄ [M]⁺: 778.3955, Found [M]⁺: 778.3954.

2.3 Synthesis of Ch-1: In a two neck flask, reflux **R-L¹** (0.3 g, 0.385 mmol) in MeOH (10 mL) at 80 °C. After **R-L¹** is completely dissolved, Dichloro(1,5-cyclooctadiene)platinum(II) (0.14 g, 0.385 mmol) is added and converted into a yellow solution. Solvents were removed using rotary evaporator. The crude product was purified via column chromatography (Al₂O₃ using Methanol 5: Dichloromethane 100). Then, the organic solvent was removed using a rotary evaporator and dried under vacuum. Yield: 42.8% (0.21 g); IR (KBr pellet): 3372, 3241, 2929, 2853, 1643, 1607, 1554, 1479, 1360, 1219, 1074, 1000, 704 cm⁻¹; ¹H NMR (500 MHz, DMSO-*d*₆) δ 8.42 (d, *J* = 7.6 Hz, 3H), 8.31 (m, *J* = 7.8, 1.5 Hz, 2H), 8.19 (d, *J* = 5.4 Hz, 2H), 7.96 (s, 2H), 7.76 – 7.67 (m, 2H), 4.22 (m, *J* = 12.7, 7.3 Hz, 2H), 4.17 – 4.09 (m, 0H), 4.11 (s, 1H), 2.20 (m, *J* = 32.6, 14.2, 7.1 Hz, 2H), 1.59 (s, 3H), 1.35 – 1.27 (m, 5H), 1.26 (d, *J* = 6.0 Hz, 3H), 0.88 (q, *J* = 7.0, 6.6 Hz, 1H); ESI-MASS (m/z) calculated for C₄₆H₅₀C₁₂N₈O₄Pt₂ [M]²⁺: 619.1314, Found [M]²⁺: 619.5035.

2.3 Synthesis of Ph-1: **Ch-1** (0.5 g, 0.382 mmol) and phenylacetylene (0.55 g, 5.34 mmol) were dissolved in distilled dichloromethane (20 mL). And diisopropylamine (0.5 mL) was added to the mixed solution. Degas the mixture by N₂ bubbling with sonication. Added a catalytic amount of copper iodide (20 mg) to the mixture. Stirred the mixture in the dark for 10 hours. A lot of water was added the reaction mixture. The product was collected by filtration and dried under vacuum to give **Ph-1** as dark brown solid in 69.9% yield (0.375 g); IR (KBr pellet): 3356, 3233, 1642, 1607, 1426, 1217, 1031, 783 cm⁻¹; ¹H NMR (500 MHz, DMSO-*d*₆) δ 9.04 (d, *J* = 5.6 Hz, 4H), 8.58 (d, *J* = 7.9 Hz, 4H), 8.41 (t, *J* = 7.9 Hz, 4H), 8.21 (s, 4H), 7.94 (d, *J* = 6.6 Hz, 2H), 7.84 (t, *J* = 6.8 Hz, 4H), 7.45 (d, *J* = 7.5 Hz, 4H), 7.37 (t, *J* = 7.5 Hz, 4H), 7.30 (t, *J* = 7.4 Hz, 2H); ESI-MASS (m/z) calculated for C₆₂H₆₀N₈O₄Pt₂ [M]²⁺: 685.2017, Found [M]²⁺: 685.4167.

2.3 Synthesis of Py-1: Pyridine (30~420 equiv.) was added to **Ch-1** solution (9 mM) in DMSO/H₂O. The mixed solution was maintained at 278 K for several days. The ligand exchange reaction by pyridine was monitored in **Ch-1** solution by ESI-MS.; ESI-MASS (m/z) calculated for C₅₆H₆₀N₁₀O₄Pt₂ [M]⁴⁺: 331.6024, Found [M]⁴⁺: 331.4167.

3. Supplementary scheme and figures



Scheme S1. Synthetic routes of **Ch-1**, **Ph-1** and **Py-1**.

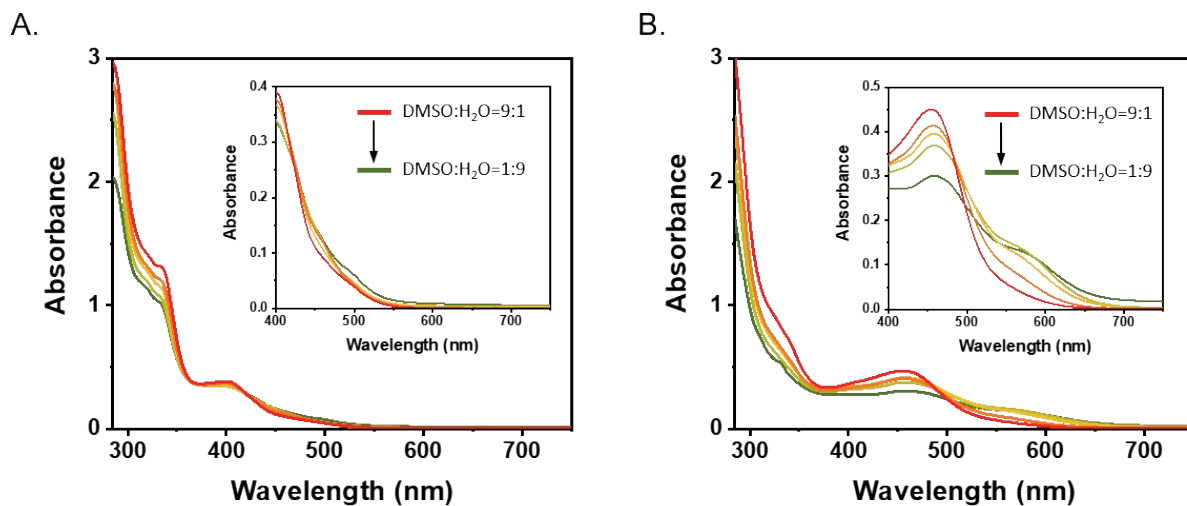


Fig. S1 UV-vis spectra of (A) **Ch-1** (9 mM) and (B) **Ph-1** (6 mM) at different composition ratios of DMSO and H₂O at 298 K.

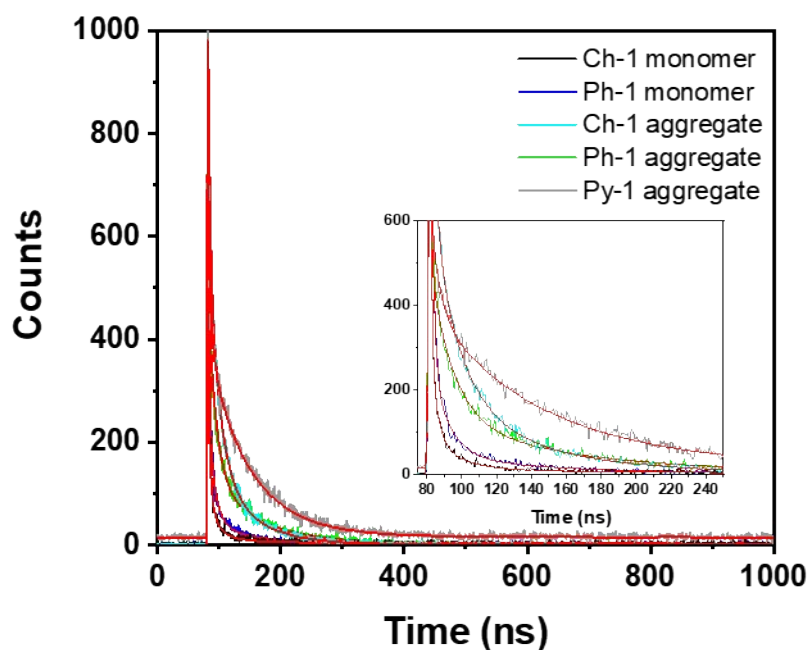


Fig. S2 Emission decay curves of **Ch-1**, **Ph-1** and **Py-1** (9 mM) in DMSO and DMSO/H₂O. All measurements were carried out at room temperature.

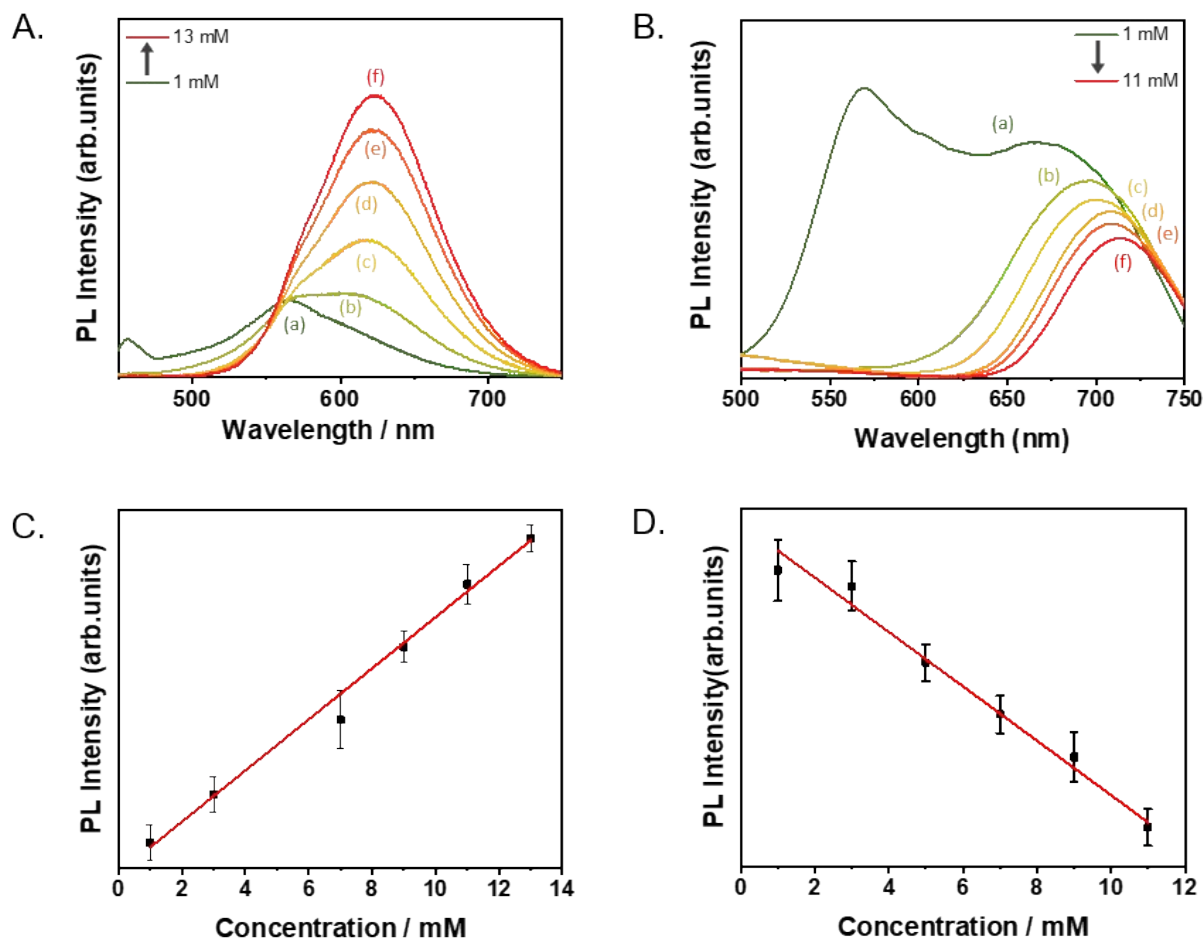
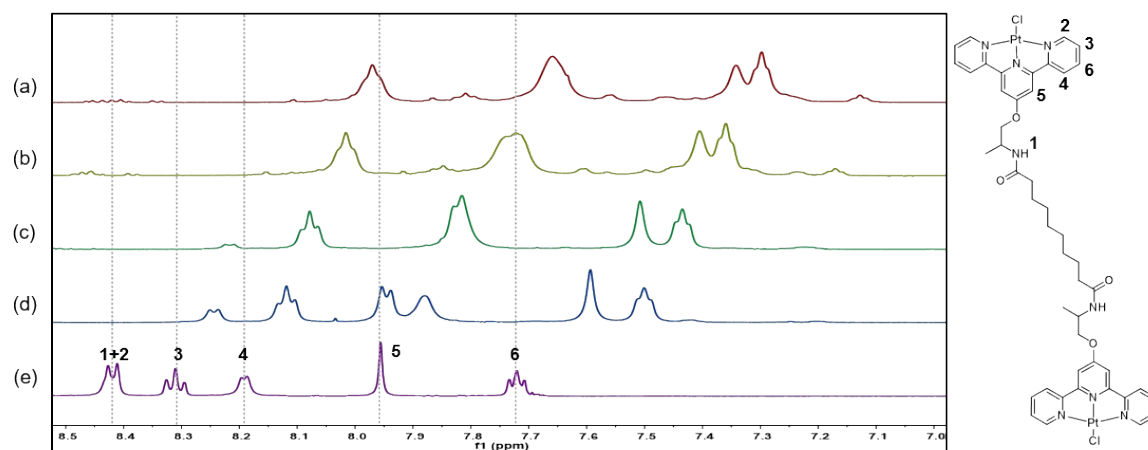


Fig. S3 Concentration-dependent PL spectra of (A) **Ch-1** and (B) **Ph-1**; (a) 1 mM, (b) 3 mM, (c) 7 mM, (d) 9 mM, (e) 11 mM and (f) 13 mM in DMSO and H₂O (1:9 v/v). (C and D) Plots of PL intensities vs. concentrations of **Ch-1** and **Ph-1** at 622.5 and 698.5 nm, respectively.

A.



B.

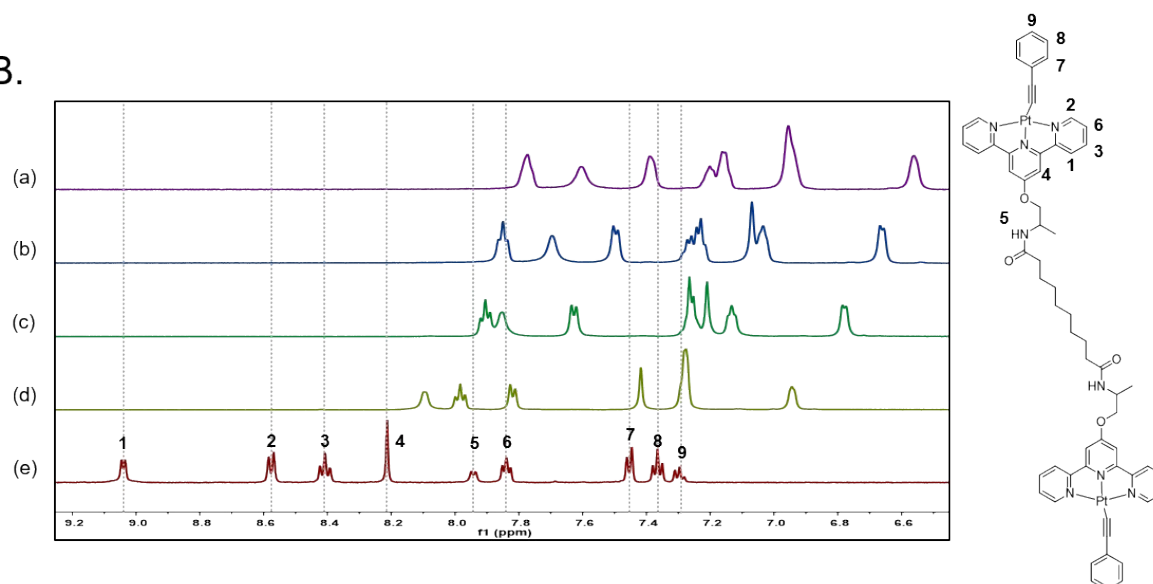
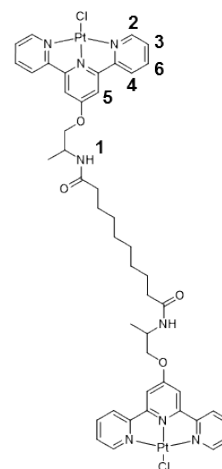
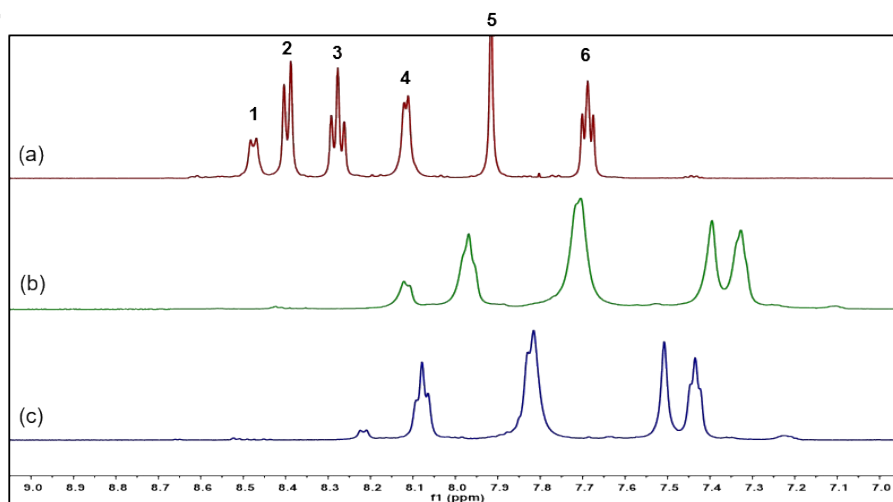


Fig. S4 ^1H NMR spectra of (A) **Ch-1** and (B) **Ph-1** by a mixed DMSO- d_6 and D_2O (a)1:9, (b)=3:7, (c)=5:5, (d)=7:3, (e)=10:0 at 323 K.

A.



B.

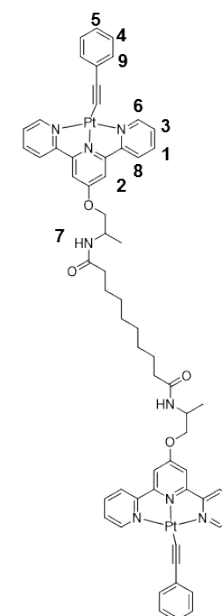
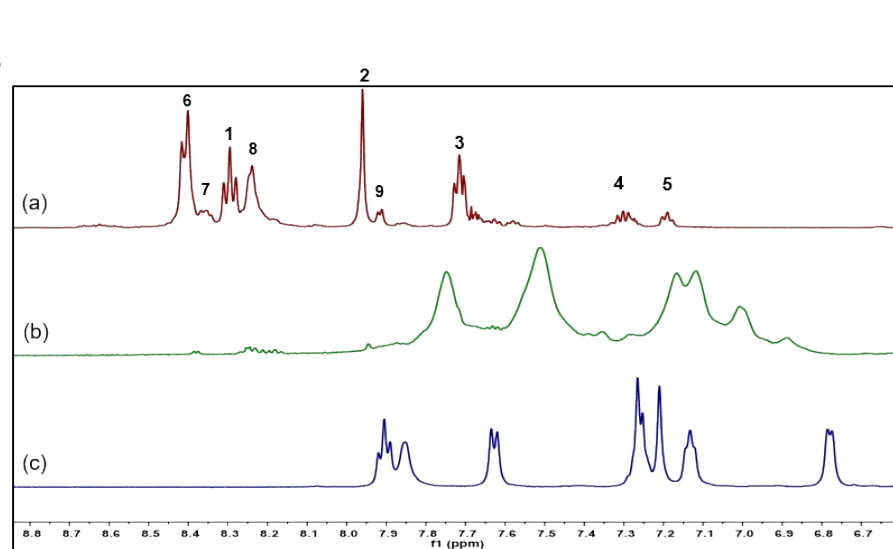


Fig. S5 Temperature-dependent ¹H NMR spectra of **Ch-1** (9 mM) and **Ph-1** (9 mM) in (a) DMSO-d₆ at 298K and (b and c) DMSO-d₆/D₂O (5:5 v/v) at (b) 298 K and (c) 323K.

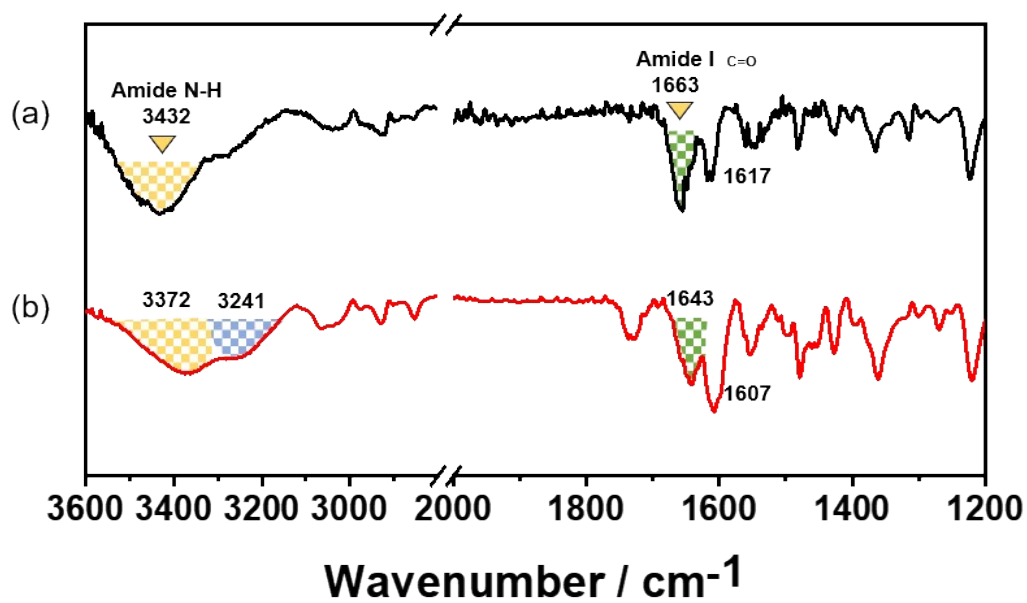


Fig. S6 FT-IR spectra of **Ch-1** (9 mM) in (a) DMSO and (b) DMSO and H₂O (1:9 v/v).

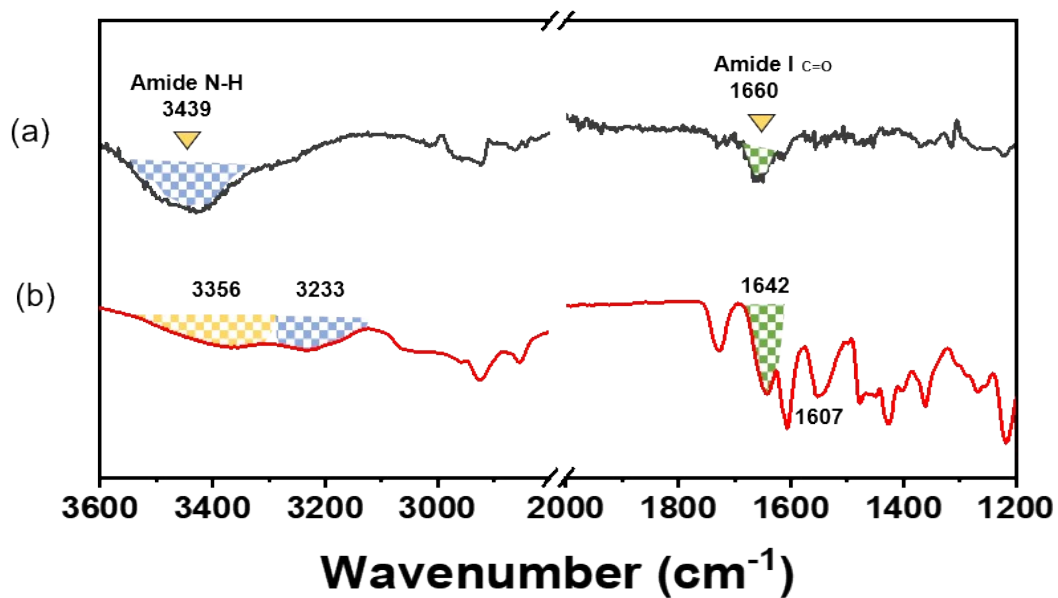


Fig. S7 FT-IR spectra of **Ph-1** (9 mM) in (a) DMSO and (b) DMSO and H₂O (1:9 v/v).

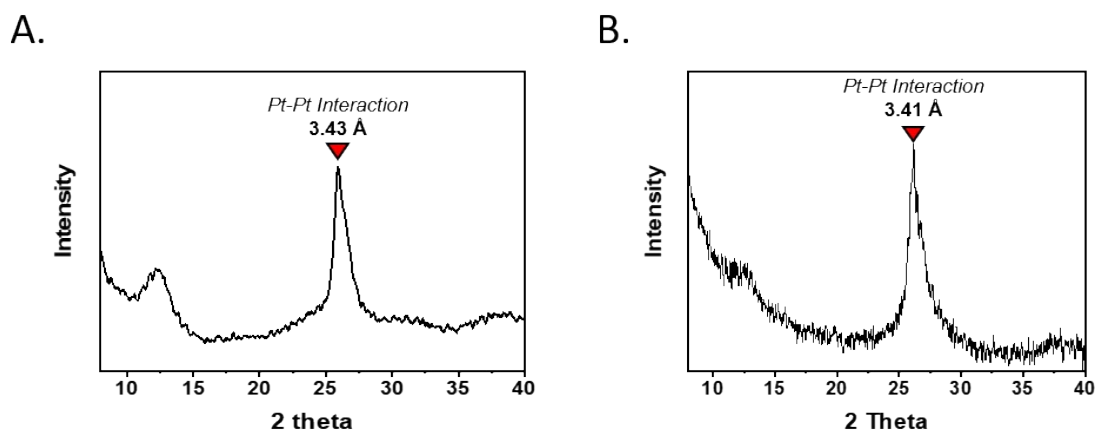


Fig. S8 WAXD patterns of (A) **Ch-1** (9 mM) and (B) **Ph-1** (9 mM) obtained in DMSO/H₂O (1:9 v/v).

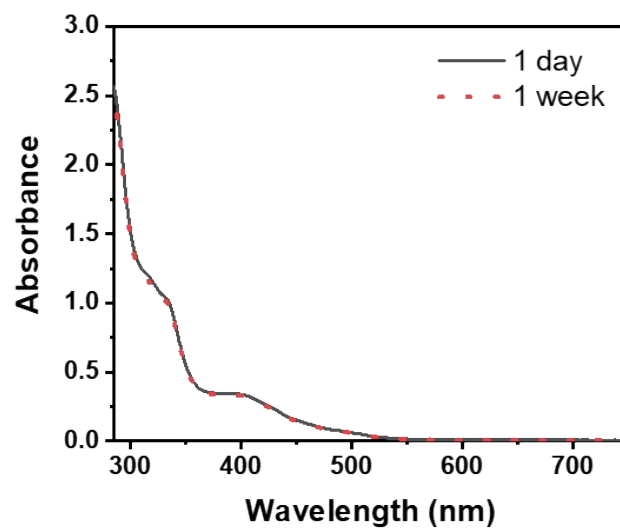


Fig. S9 UV-vis spectra of **Ch-1** after aging time for 1 day and 1 week.

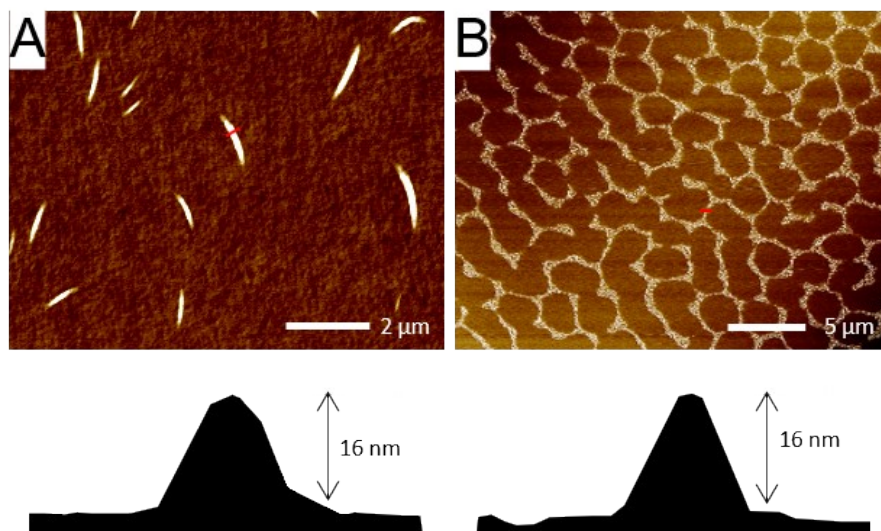


Fig. S10 AFM images and height profiles of **Ch-1** after aging time for (A) 1 day and (B) 5 days.

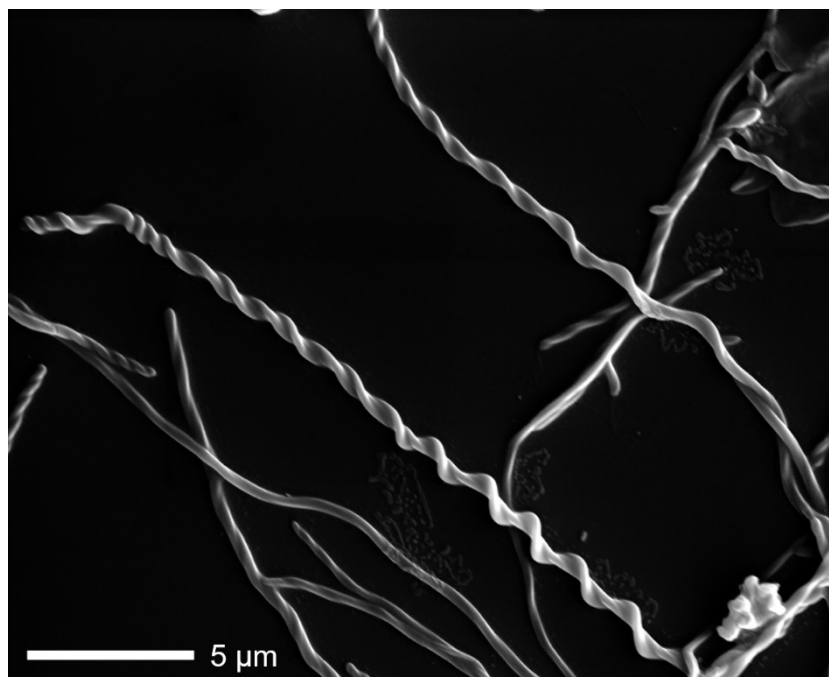


Fig. S11 SEM image of **Ph-1** (9 mM) obtained from DMSO and H₂O (1:9 v/v).

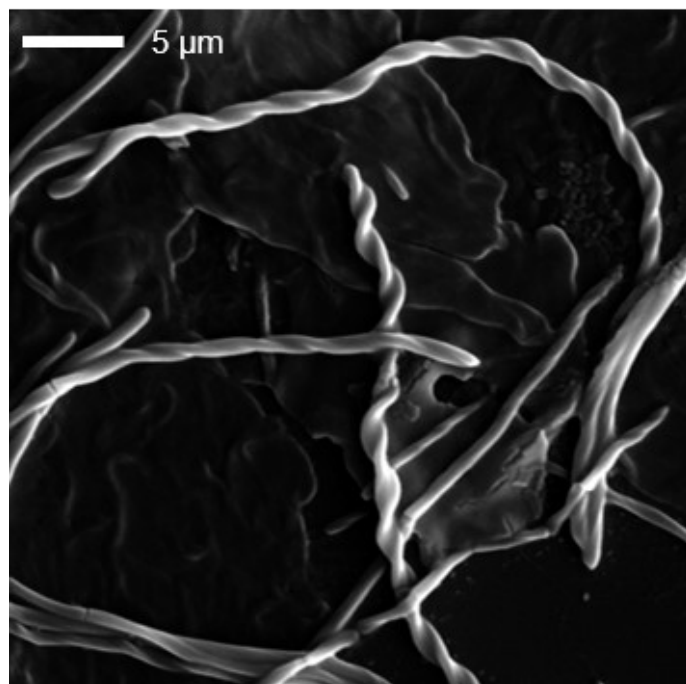
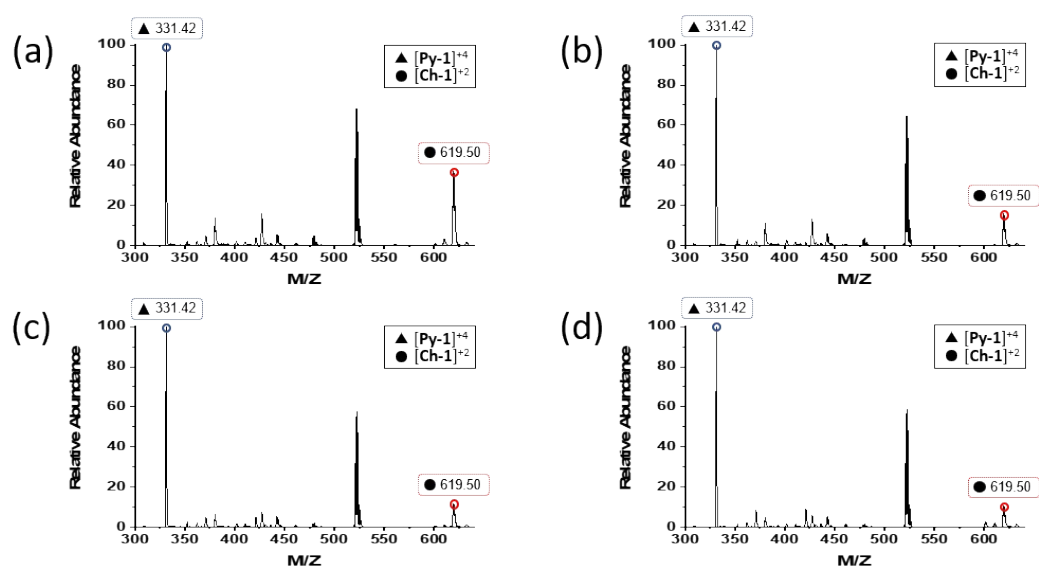


Fig. S12 SEM image of **Ph-1** (9 mM) after aging time for 1 week.

A.



B.

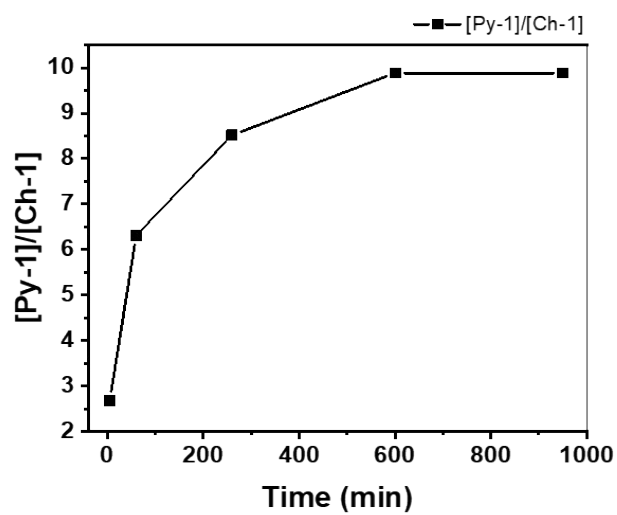


Fig. S13 ESI-MS spectra of **Ch-1** (9 mM) (A) upon addition of pyridine 140 equiv. (a) 5 min, (b) 1 hours, (c) 4 hours, (d) 10 hours. (B) Plot for time vs intensity of **Py-1/Ch-1**.

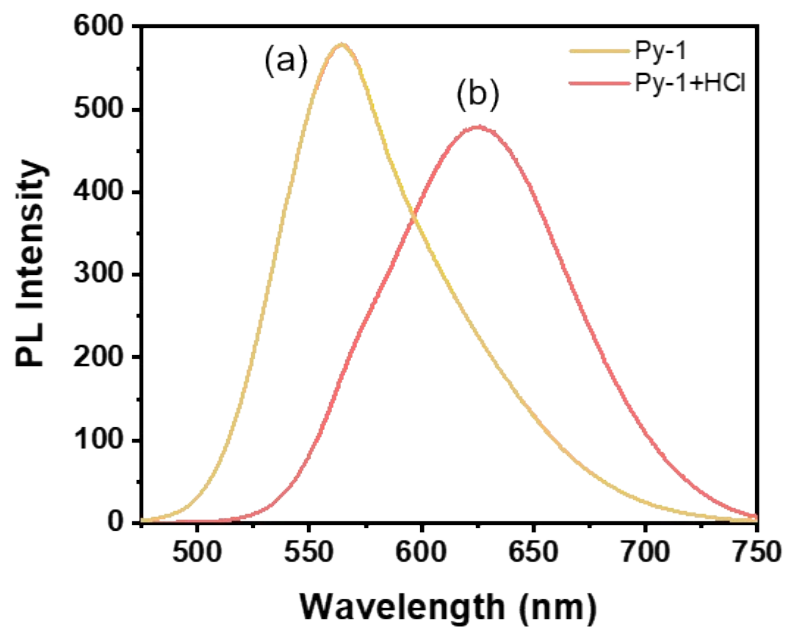


Fig. S14 PL spectra of (a) **Py-1** (9 mM) upon addition of (b) HCl (140 equiv.) in DMSO and H₂O (1:9 v/v).

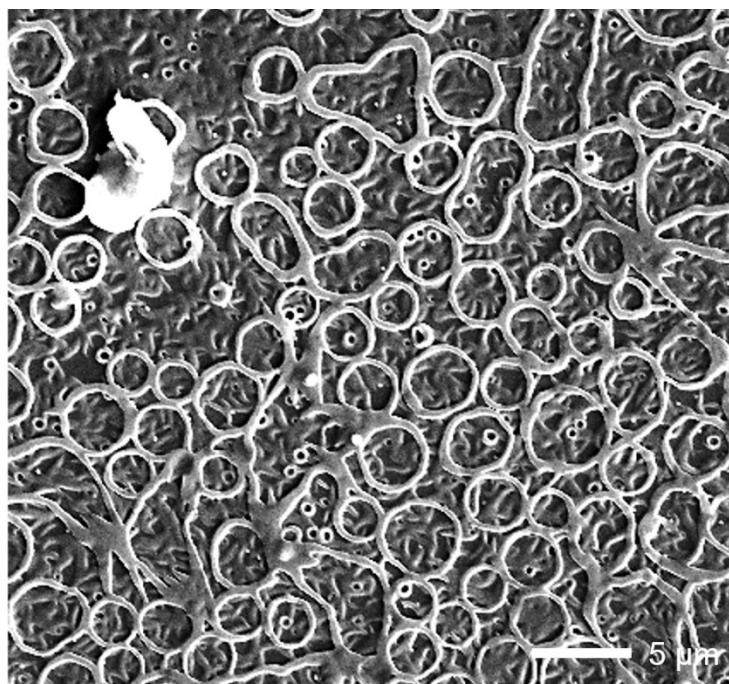


Fig. S15 SEM image of Py-1 upon addition of HCl (140 equiv.) in DMSO and H₂O (1:9 v/v).

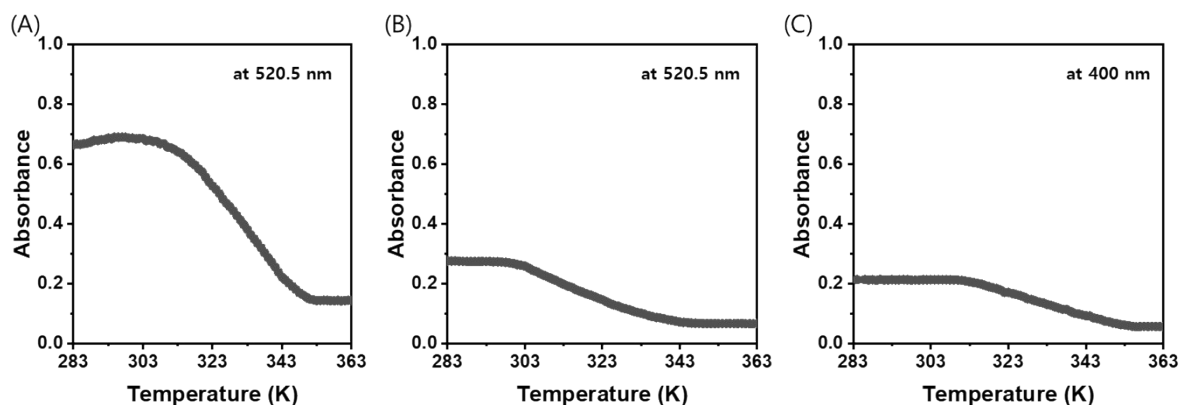


Fig. S16 Plot of absorbance of (A) **Ch-1**, (B) **Ph-1**, and (C) **Py-1** in DMSO/H₂O (1:9 v/v) as function of temperature observed during heating processes from 363 to 283 K (at rate of 1K min⁻¹)

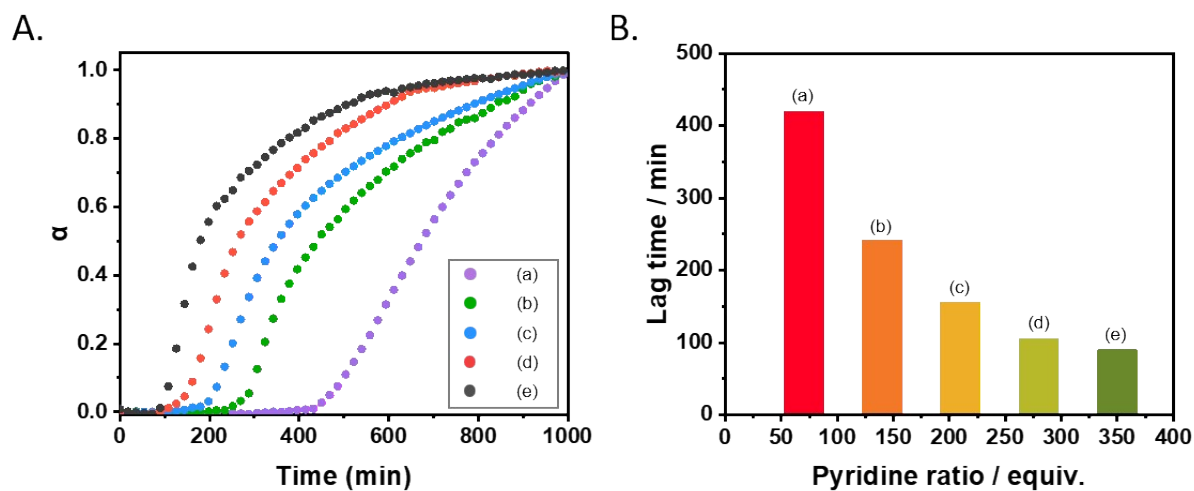


Fig. S17 (A) Plot for α_{agg} of **Ch-1** (9 mM) at different concentrations of pyridine vs. time in DMSO and H₂O (1:9 v/v). (B) Plot for concentration of pyridine vs. lag time. (a) 70 equiv., (b) 140 equiv., (c) 210 equiv., (d) 280 equiv., (e) 350 equiv.

Table S1. Luminescence lifetimes of **Ch-1** (9 mM) and **Ph-1** (9 mM) in DMSO and H₂O (1:9 v/v) or DMSO.

	Solvent (DMSO:H₂O v/v)	Aveg. Lifetime (nS)
Ch-1	DMSO	18.7
Ph-1	DMSO	25.3
Ch-1	DMSO:H₂O (1:9 v/v)	36.3
Ph-1	DMSO:H₂O (1:9 v/v)	56.4
Py-1	DMSO:H₂O (1:9 v/v)	60.8

Table S2. Thermodynamic parameters of **Ch-1**, **Ph-1** and **Py-1** obtained in DMSO and H₂O (1:9 v/v).

	ΔH_c (kJ mol ⁻¹)	ΔS (J K ⁻¹ mol ⁻¹)	T_c (K)	ΔG (kJ mol ⁻¹)	K_c (L mol ⁻¹)
Ch-1	-120.0	-323.62	330.78	-25.18	3 x 10⁴
Ph-1	-110.46	-312.95	313.71	-18.77	2.2 x 10³
Py-1	-126.14	-342.17	328.03	-25.88	4.1 x 10⁴

4. Analytical data

4.1 ^1H -NMR and ^{13}C -NMR spectroscopy

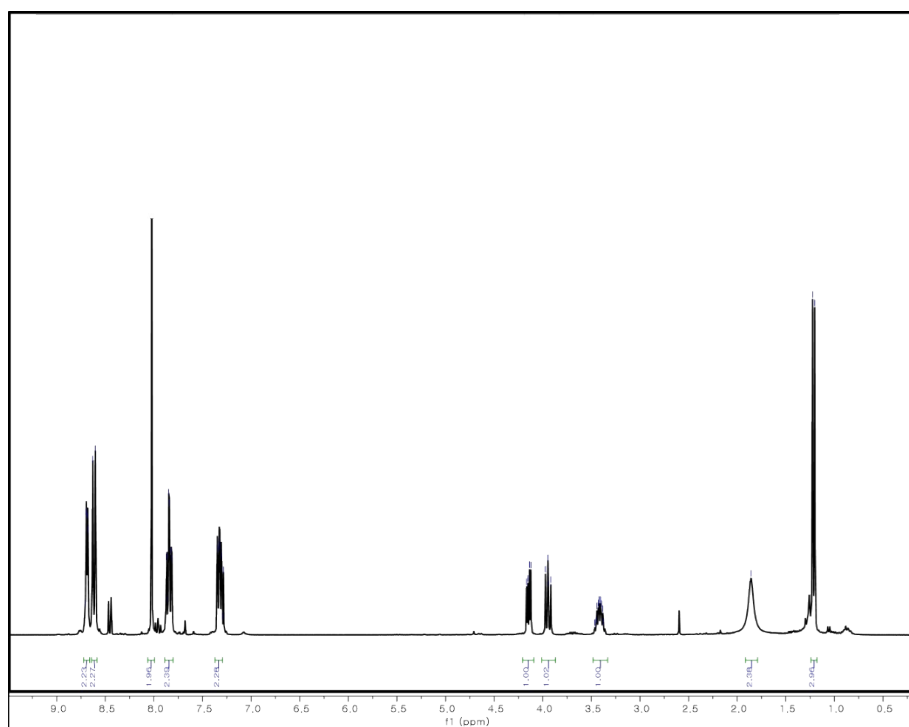


Fig. S18 ^1H NMR spectrum (300 MHz) of $R\text{-L}^2$ in CDCl_3 at 298 K.

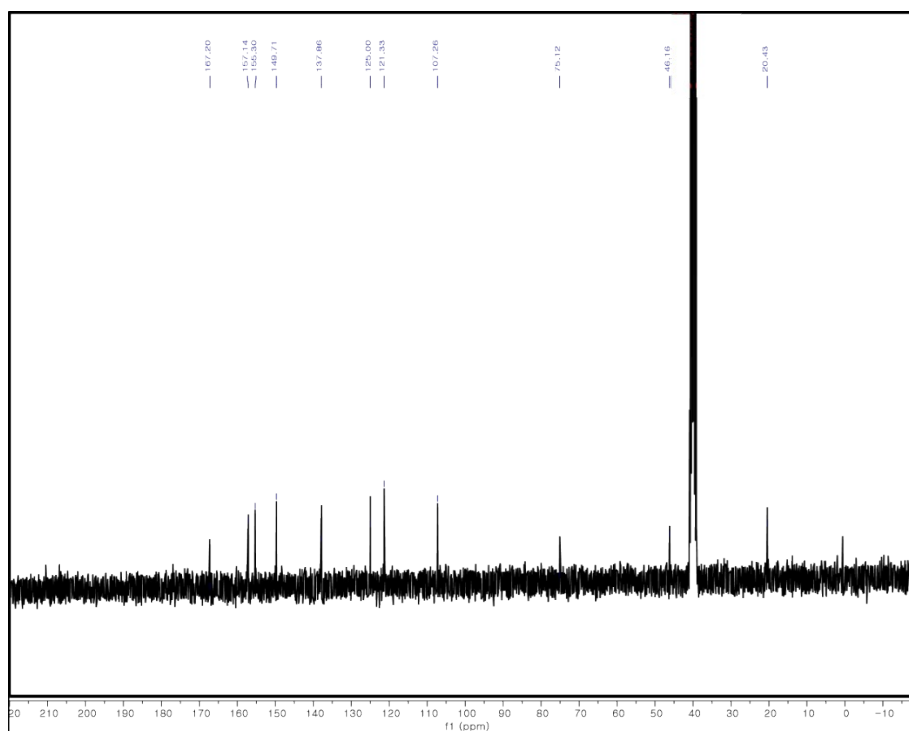


Fig. S19 ^{13}C NMR spectrum (75 MHz) of $R\text{-L}^2$ in $\text{DMSO-}d_6$ at 298 K.

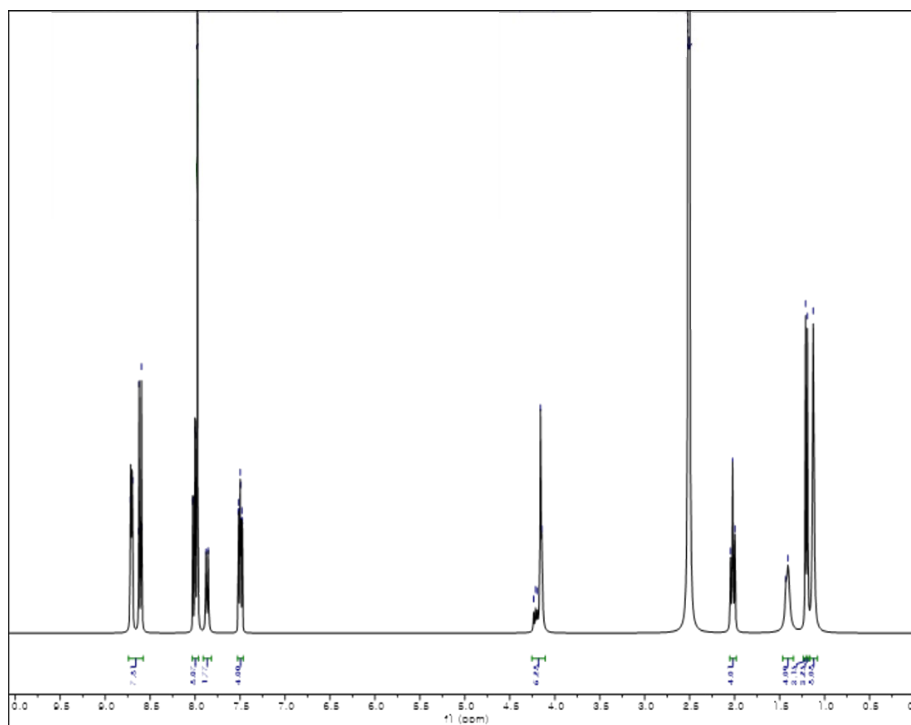


Fig. S20 ^1H NMR spectrum (300 MHz) of $R\text{-L}^1$ in $\text{DMSO-}d_6$ at 298 K

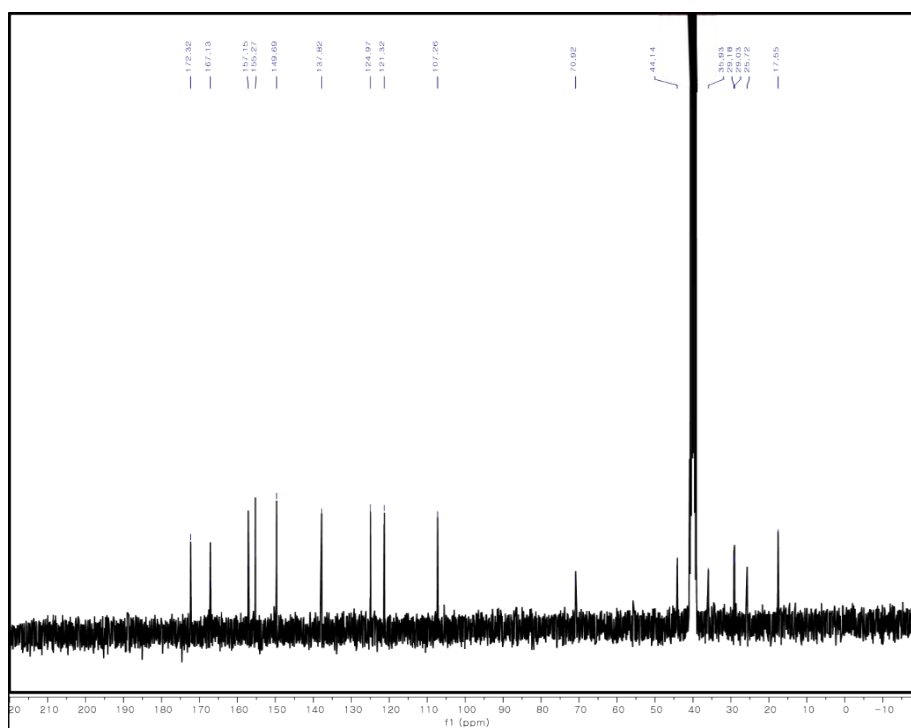


Fig. S21 ^{13}C NMR spectrum (75 MHz) of $R\text{-L}^1$ in $\text{DMSO-}d_6$ at 298 K.

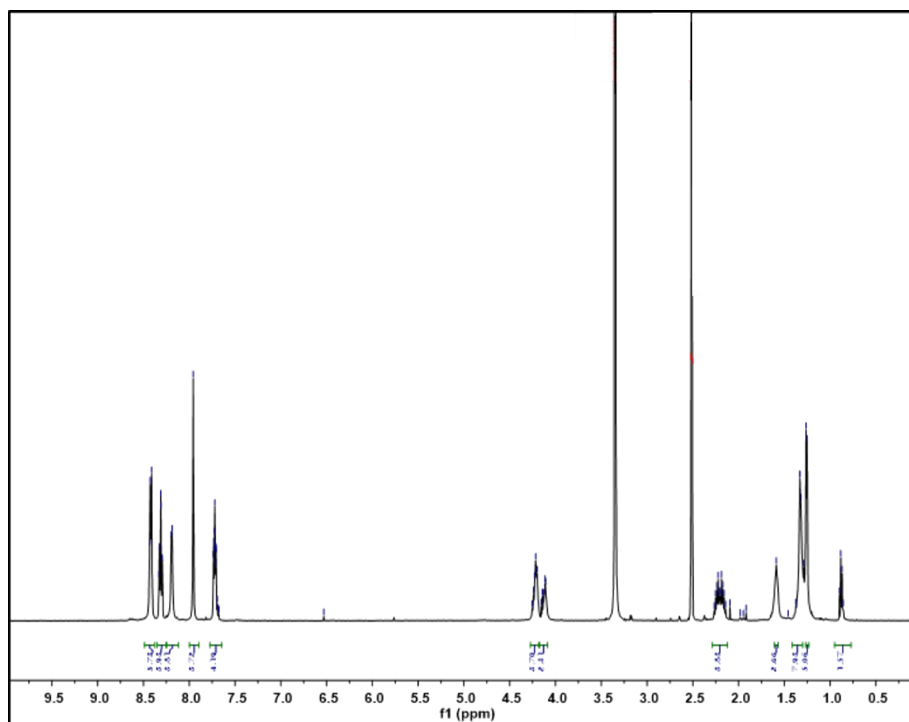


Fig. S22 ^1H NMR spectrum (300 MHz) of **Ch-1** in $\text{DMSO-}d_6$ at 298 K.

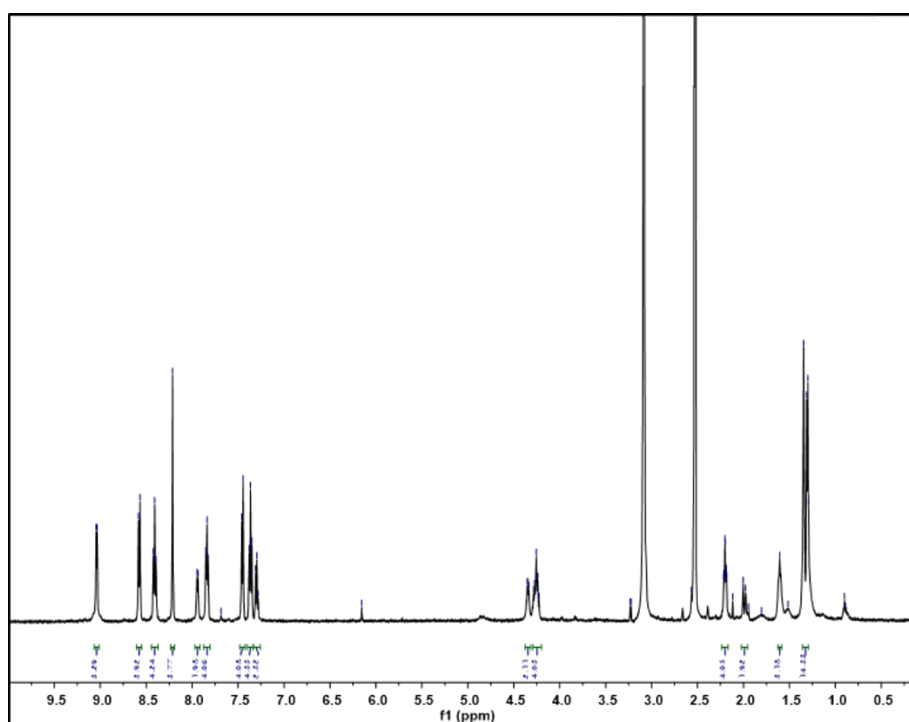


Fig. S23 ^1H NMR spectrum (500 MHz) of **Ph-1** in $\text{DMSO-}d_6$ at 353 K.

4.2 HR and ESI mass spectrometry

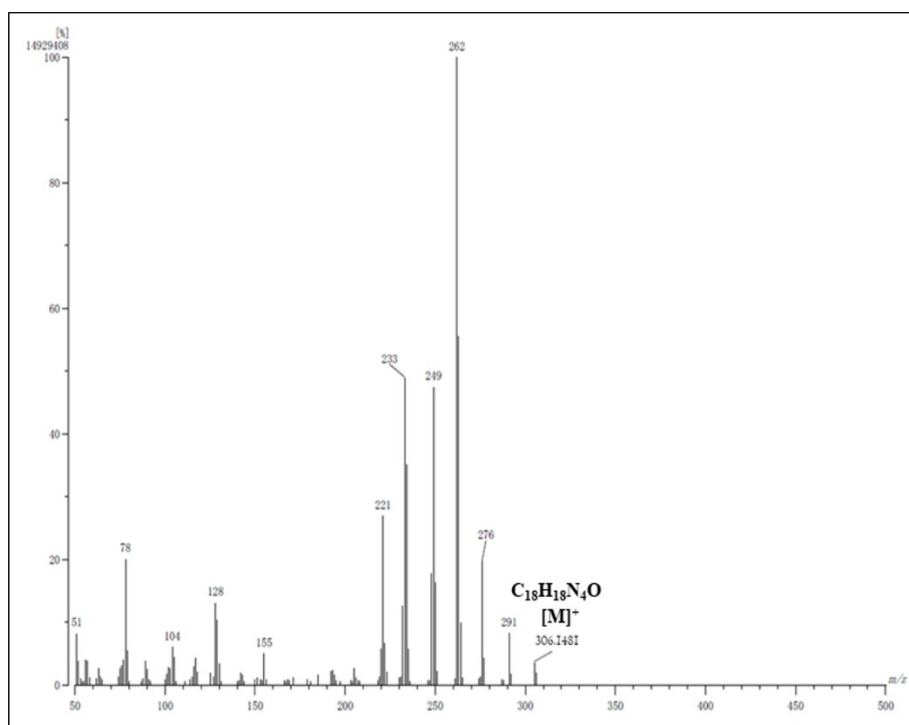


Fig. S24 HR EI-MS spectrum of $R-L^2$ in DCM.

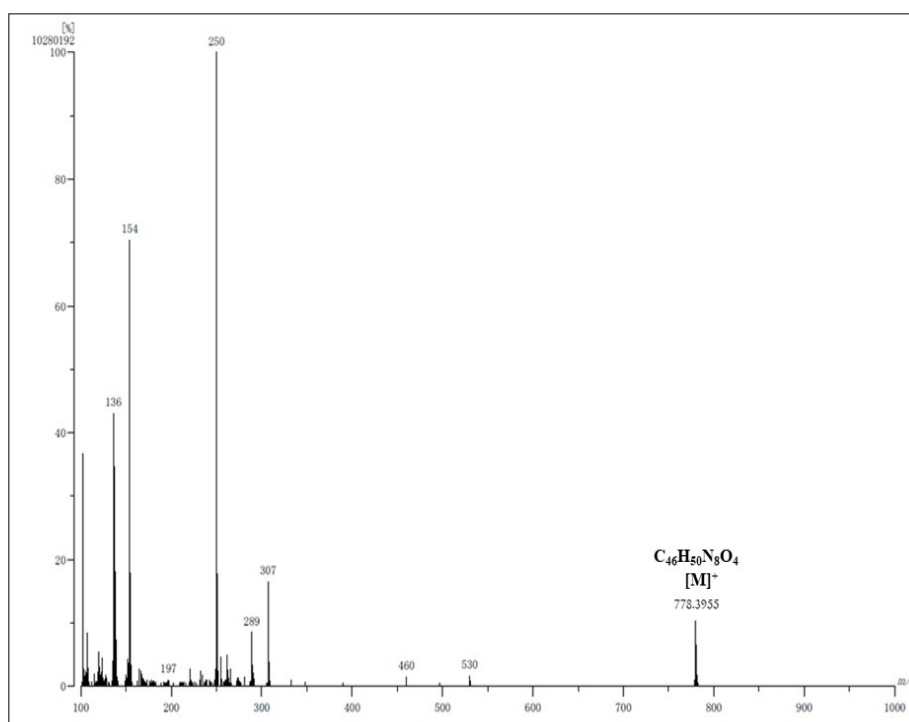


Fig. S25 HR FAB-MS spectrum of $R-L^1$ in DCM.

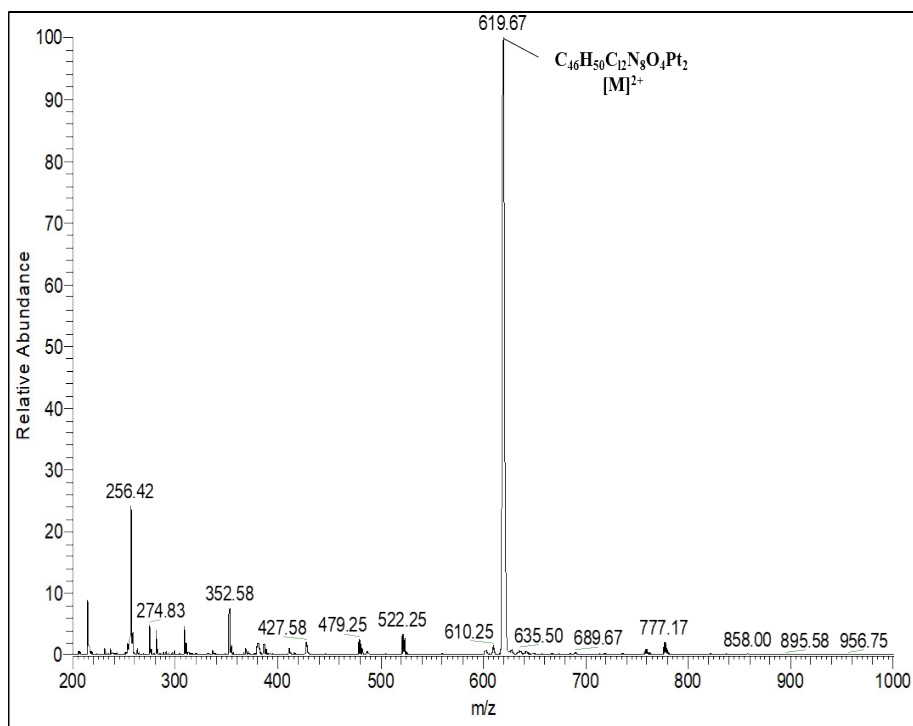


Fig.S26 ESI Mass spectrum of **Ch-1** in H₂O.

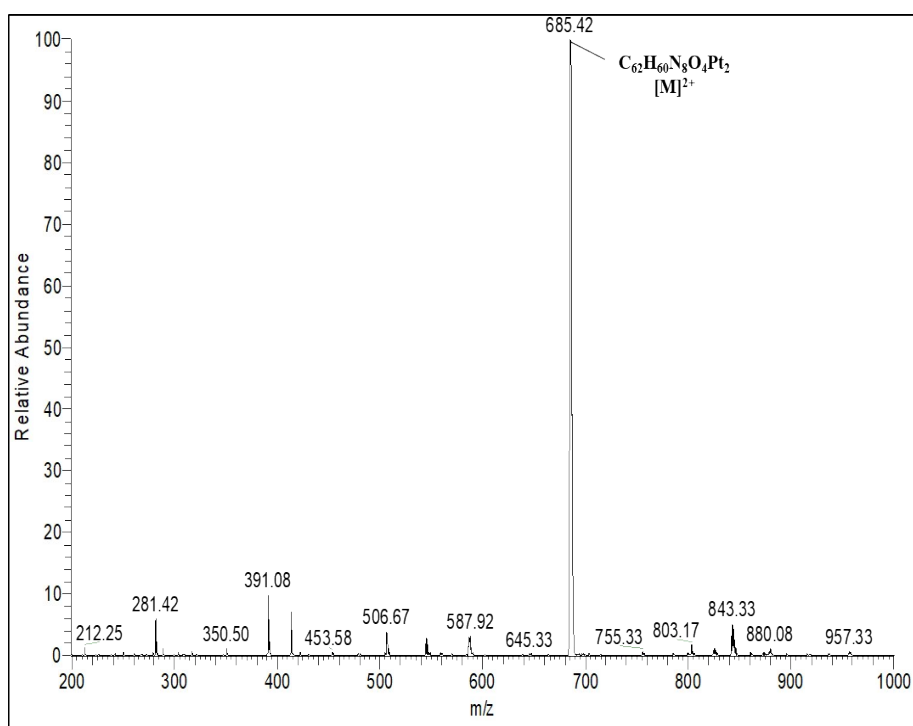


Fig.S27 ESI Mass spectrum of **Ph-1** in MeOH.

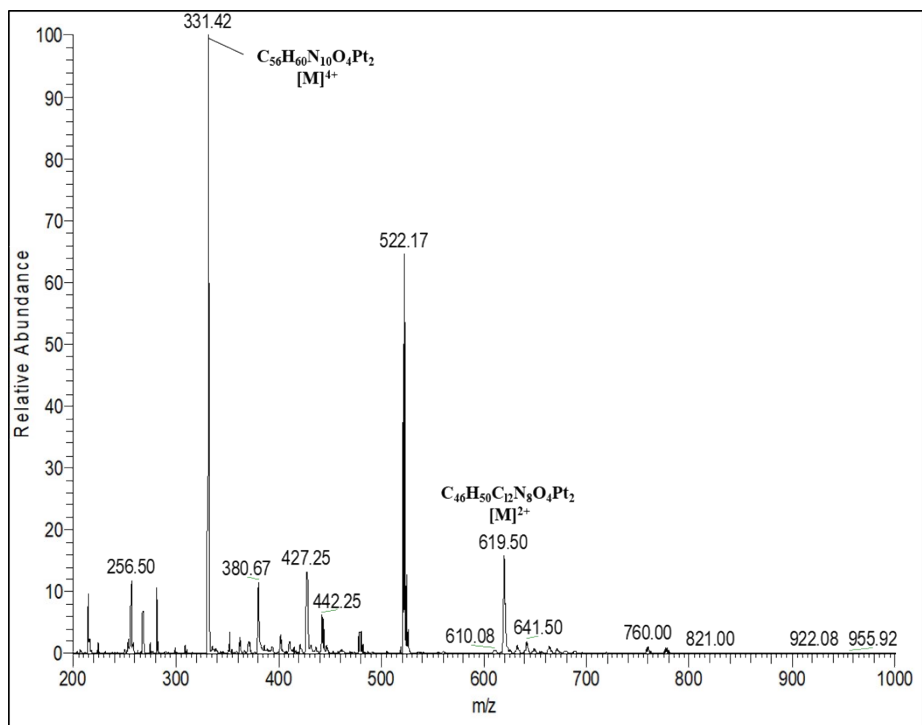


Fig.S28 ESI Mass spectrum of **Py-1** in H₂O.

Notes and references

1. H. M. M. ten Eikelder, A. J. Markvoort, T. F. A. de Greef and P. A. J. Hilbers, *J. Phys. Chem. B*, 2012, **116**, 5291-5301.
2. M. M. J. Smulders, M. M. L. Nieuwenhuizen, T. F. A. de Greef, P. van der Schoot, Schenning, A. P. H. J. Meijer, E. W., How to distinguish isodesmic from cooperative supramolecular polymerisation. *Chem. Eur. J.* **2010**, *16* (1), 362-367.
3. H. Choi, S. Ogi, N. Ando, S. Yamaguchi, Dual trapping of a metastable planarized triarylborane π -system based on folding and lewis acid–base complexation for seeded polymerization. *J. Am. Chem. Soc.* **2021**, *143* (7), 2953-2961.
4. M. H.-Y. Chan, M. Ng, S. Y.-L. Leung, W. H. Lam, Yam, V. W.-W., Synthesis of luminescent platinum(II) 2,6-bis(N-dodecylbenzimidazol-2'-yl)pyridine foldamers and their supramolecular assembly and metallogel formation. *J. Am. Chem. Soc.* **2017**, *139* (25), 8639-8645.